Comparison of Front-Tracking and Front-Capturing Computations with Experimental Images of Drop Impact onto Shallow Liquid Pools

Y. Hardalupas *, H. Pergamalis * and A.M.K.P. Taylor *
G.E. Cossali and M. Marengo****
h.pergamalis@ic.ac.uk, marengo@unigb.it

*** Imperial College of Science, Technology and Medicine,**
Mechanical Engineering Department,
London SW7 2BX, UK
**** Università degli Studi di Bergamo**
Facoltà di Ingegneria
24044 Dalmine (BG) - Italy

Abstract

This paper compares the ability of two different flow-model/computational-method combinations to predict qualitatively the evolution of the free-surface, and in particular the shape of the crown formed during the impingement event of a single droplet onto shallow liquid pools. A one-fluid inviscid model, solved by a Boundary-Integral-based front-tracking method and a two-fluid viscous model, run on a commercial CFD platform featuring front-capturing capabilities, are tested. Time-resolved experimental images of the phenomenon are used as the comparison benchmark. The example case presented in this paper involves the impingement of a Ø3.85mm water drop onto a quiescent, 1.12mm-deep water pool with 3.05m/s. Both computational approaches capture the most important axisymmetric characteristics of the impact process, such as the initial ejection of a lamella and its subsequent growth into a curved crown with a characteristic rim on its edge. The effects of viscosity on the evolution of the impingement event are found to be negligible in most flow regions bar the upper part of the crown.

Introduction

Drop impingement onto wetted surfaces is encountered in both natural and engineering processes. Examples include, among many others, raindrop-induced soil erosion and spray-painting, respectively. It is well known that the development of the flow during the impingement event involves a considerable amount of highly-transient free-surface deformation; a crown will form [1,2], accompanied by the ejection of satellite droplets from its free rim [3,4]. Currently, prediction of the evolving shape of the gas/liquid interface is only possible by numerical means. To this end, employment of computational techniques featuring either front-tracking or front-capturing capabilities becomes necessary [5]. Front-tracking involves direct assignment of computational nodes onto the interface. Lagrangian advection of the nodes during the course of the computation allows explicit knowledge of interface topology. This approach, however, may require considerable algorithmic overheads when full three-dimensional simulations are attempted or the resolution of complex topological changes such as interface detachment or reconnection is desired [6]. On the other hand, front-capturing methodologies do not attempt to track interfaces explicitly. The locus of the interface is reconstructed within a Eulerian finite-volume grid using the instantaneous distribution of an advected volume-fraction indicator quantity, instead [5]. This approach inherently caters for complex topological changes, although relatively high grid densities may be required for the maintenance of a sharp interface.

Front-tracking methodologies have proven a popular choice for the numerical investigation of a number of free-surface flow problems, ranging from bubble motion [7] and drop oscillations in zero gravity [8] to wave motion [9] and dam-breaking flows [10], particularly when implemented in conjunction with a Boundary-Integral Method (BIM). The main advantage of BIM-based formulations lies in the relatively substantial computational savings they can offer. These are realized by conversion of a problem's governing differential equations into their Boundary-Integral equivalent form. This allows the computational effort to be concentrated on the problem's boundaries (or surface), without further numerical consideration for the underlying bulk fluid motion. The disadvantage of BIM formulations is that only incompressible, inviscid and irrotational [7-10], or highly-viscous [11] flows in two dimensions may be considered, since the full three-dimensional Navier-Stokes and conservation equations cannot be mathematically converted into a pure Boundary Integral form. Nevertheless, several studies of different aspects of the drop impact problem have been successfully carried out using BIM-based front-tracking methodologies.

Oguz and Prosperetti [12] investigated the behaviour of the liquid bridge connecting an impacting drop to a curved target liquid surface during the first instances after impact. Their calculations predicted the entrapment of miniscule toroidal bubbles between the contacting surfaces. Entrainment of such bubbles has also been observed in experimental studies of vortex ring shedding during drop impact onto deep liquid pools [13]. Prosperetti and Oguz [14] also studied the mechanism by which larger bubbles are entrapped by the impact of raindrops onto the surface of the ocean, leading to the generation of underwater sound. Their calculations demonstrated the entrapment process to be heavily dependant upon a delicate balance between the timing of the collapse of the liquid crater walls formed subsequent to the impact, and showed good agreement with experimental evidence. More recently, Weiss and Yarin [15] showed that the formation of a liquid crown during the impingement of a droplet onto a thin liquid film may also be captured by BIM-based front-tracking computations. However, and owing to the lack of further comparison with experimental evidence therein, correct qualitative prediction of the *shape* of the crown by the particular flow-model/numerical-method approach employed [15], is still questionable.

One of the aims of the present work is to examine the ability of a one-fluid, potential flow model, solved numerically by a Boundary-Integral-based front-tracking method, to predict the shape of the crown during its initial development and later propagation in the case of drop impingement onto a wetted surface. To this end, time-resolved experimental images of a water drop impinging onto a shallow water pool are used as a qualitative comparison benchmark. Additionally, the numerical results obtained are further compared and contrasted to fully viscous and incompressible two-fluid computations performed with the commercially-available *Comet*™ CFD package, which features a front-capturing capability included specifically for tackling free-surface problems. The aims of this exercise are to investigate the ability of such an off-the-shelf package, as opposed to a purpose-written research code, to tackle the droplet-impact/crown formation problem and compare the performance of the featured front-capturing scheme with that of the front-tracking scheme, in the light of the computational resource requirements of each implementation.

Experimental Technique

Single liquid drops were produced by a vertically-suspended needle, connected to a feeding tank *via* a solenoid valve. Drop detachment was instigated by a small pressure pulse, created by briefly opening the valve. Drop diameters, *D*, were measured from enlarged images to have an average value of 3.82mm, with a production repeatability of 94% or higher. The drops were left to free-fall from a variety of heights ranging from 300mm to 900mm above the surface of a target pool of liquid placed directly underneath the needle. The impact velocities, *U*, ranged from 2.3m/s to 4.2 m/s. The pool was produced by sticking a thin aluminium ring (Ø>50 mm) onto a plate of glass and filling the enclosed region. The pool's thickness, *h*, was varied from 1.1 mm to 4.3 mm, and a drain was employed to keep it constant in view of the accumulation of liquid due to the impingement of several drops during experimentation. A CCD camera (PCO Flashcam, resolution 752x286 pixels), combined with a 10μs-duration flash lamp, was used to capture the phenomenon at different times after impact. The flash was triggered via a delay circuit by the passage of the falling drops through a laser beam directed onto a photodiode. The present example case concerns the impingement of a Ø3.85mm water drop onto a 1.12mm-deep water pool with an impact speed is 3.05m/s.

BIM Front-Tracking Approach

The present BIM-based front-tracking methodology is similar to that described in [15]. An axially-symmetric, incompressible, inviscid and irrotational unsteady flow model is adopted. The effects of the surrounding air on the motion of the free-surface are neglected, with computations being consequently performed for the liquid side of the air/water system only. The effects of surface-tension and gravity are, however, taken into account. The system of governing equations comprises the mass-conservation equation, re-expressed in terms of the velocity potential, ϕ as:

$$\nabla^2\Phi = 0 \tag{1}$$

and the unsteady Bernoulli-integral equation:

$$\frac{\partial\Phi}{\partial t} = -\frac{\nabla\Phi^2}{2} - gz - \frac{1}{\rho}P \tag{2}$$

where g is the acceleration of gravity, ρ the liquid density and P the liquid pressure. In view of the experiments, a spherical water drop, of radius *R*, is considered to impinge onto the surface of a circular quiescent pool of water, of depth *h*, at right angles with a uniform speed, *U*. Rigid smooth walls bound the pool along its bottom and side. Owing to the assumption of axisymmetry and the adoption of a BIM, the computational domain corresponding to this initial geometry is effectively reduced to the curvilinear boundary of its half-meridian generator plane (*see* Fig. 1). Similarly to [12], [14] and [15], the droplet is initially taken to be attached to the pool surface, since the front-tracking method implemented here does not support reconnecting interfaces. A portion of the drop's bottom, typically 5% of the droplet's diameter, is removed and the now finite connection locus, or "neck", is smoothed-out by a circular fillet to avoid initial topological singularities. Figure 1 summarises the initial geometry and boundary conditions [15]. In the computations, all lengths are normalised by the drop's initial radius, *R*, and all velocities by *U*.

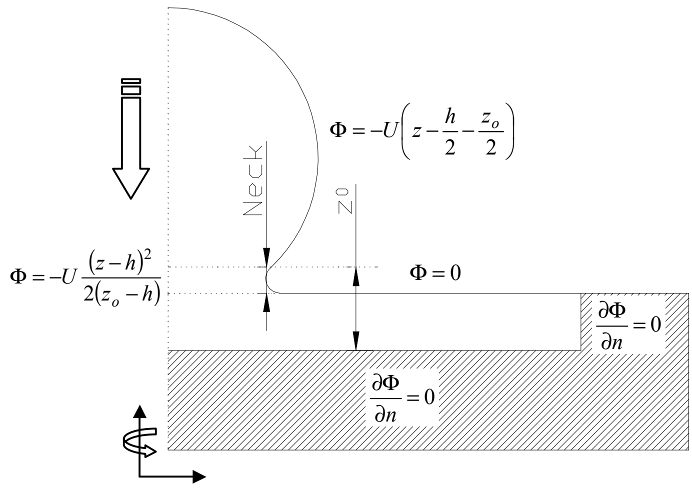

Figure 1. Schematic summary of the initial boundary geometry and conditions employed for the BIM-based front-tracking computations.

During the course of the calculation, Equations (1) and (2) are solved on the liquid domain's boundary only. Equation (1) is first transformed into its Boundary-Integral equivalent and then solved by a standard BIM technique [16]. A linear isoparametric boundary-element discretisation scheme is employed, where two boundary nodes are used to define each element. For each computational step, the BIM solution yields the velocity of the fluid normal to the free-surface. This allows its advection to a new spatial *locus*. The velocity potential on the free-surface, needed for the BIM solution of the next step, is updated by integration of the Lagrangian equivalent of Equation (2) in time. An upper-bounded Euler time-stepping scheme is employed for all temporal integrations. To avoid stiffness, periodic re-distribution of the free-surface nodes is carried out, with the aim of keeping the global boundary-element length uniform. The pressure term of Equation (2) is a function of the curvature of the free-surface, which is approximated in a smooth fashion with the aid of cubic splines fitted through the series of boundary-element end-nodes. The code developed was executed on a 1GHz-class Athlon™ processor-based Windows™ desktop PC with 256Mb of RAM. Convergence studies showed boundary grid densities greater than 24 elements per dimensionless unit length to yield qualitatively identical solutions at large times after impact. For this level of interface resolution, and the radius of the pool set at 6 dimensionless units, a total of 346 boundary elements (of which 193 were assigned to the free-surface, the rest defining the bounded domain surfaces) and a maximum timestep of 0.5μs were necessary to perform the computations presented herein. The run required 1.89MB of memory and approximately 6s of total run-time per iteration.

Front-Capturing Approach

The front-capturing computations were performed on the commercially-available *Comet*™ CFD package. Similarly to the front-tracking method described above, an axially-symmetric and incompressible unsteady flow model was chosen. However, the flow was set to be viscous, while the effects of the surrounding gaseous phase on the evolution of the gas/liquid interface were taken into account, as were the effects of surface-tension and gravity. The featured 'High Resolution Interface Capturing' (HRIC) scheme was used to reconstruct the interface from the distribution of an advected colour function. The colour function's initial distribution, as well as the corresponding fluid kinematic conditions, were specified by a purpose-written user subroutine to give *identical* initial conditions to those utilised for the front-tracking implementation, for the sake of comparison. In view of the axisymmetric geometry assumed, the computational grid employed was a 1°-wide cylindrical sector (wedge) with a circumferential cross-section of 50mm x 50mm in height and radius, respectively. Smooth solid wall boundary conditions were assigned to all boundary cell faces. Cell sizes were gradually refined towards the datum of the domain, with the largest cells set in the gaseous phase near the domain boundaries, and the smallest within -and adjacent to- the initial locus of the liquid phase. Convergence studies showed that unacceptable interface diffusion occurred when cell sizes greater than 50μm square were assigned to the latter regions. In view of this, cells below to 2.5 μm were used, giving a total of 343510 for the example case presented here. A timestep of 2μs was used for the present computations. *Comet*™ was executed on a Unix HP J282 9000/780 workstation, featuring a 180MHz RISC processor and 1GB of RAM. The run presented here took about 130s per step (100% CPU time).

Results and Discussion

Time-resolved images of the impingement event are presented in the left column of Fig. 2, along with the shapes of the free-surface predicted by the front-tracking and front-capturing computations, in the centre and right column, respectively. The impingement event is conveniently considered to commence upon the first contact of the drop onto the pool's surface, in order to facilitate comparison with the simulations. It must be noted that, in practice, it is difficult to determine the exact moment of first contact unambiguously; the first image of Fig. 2 depicts the drop to have already established a small but finite contact footprint. At 0.1ms, the experimental image depicts the commencement of ejection of a circumferential liquid lamella. Both computational methods capture this, although the BIM predicts a thicker lamella owing to the use of lower (in absolute dimensional terms) interface resolution. The employment of a minimum boundary element size is dictated by the need to avoid the capture of toroidal bubble entrapment during the initial stages of impact [12,13,15], beyond which the present computation cannot proceed since special treatment for reconnecting interfaces is not provided.

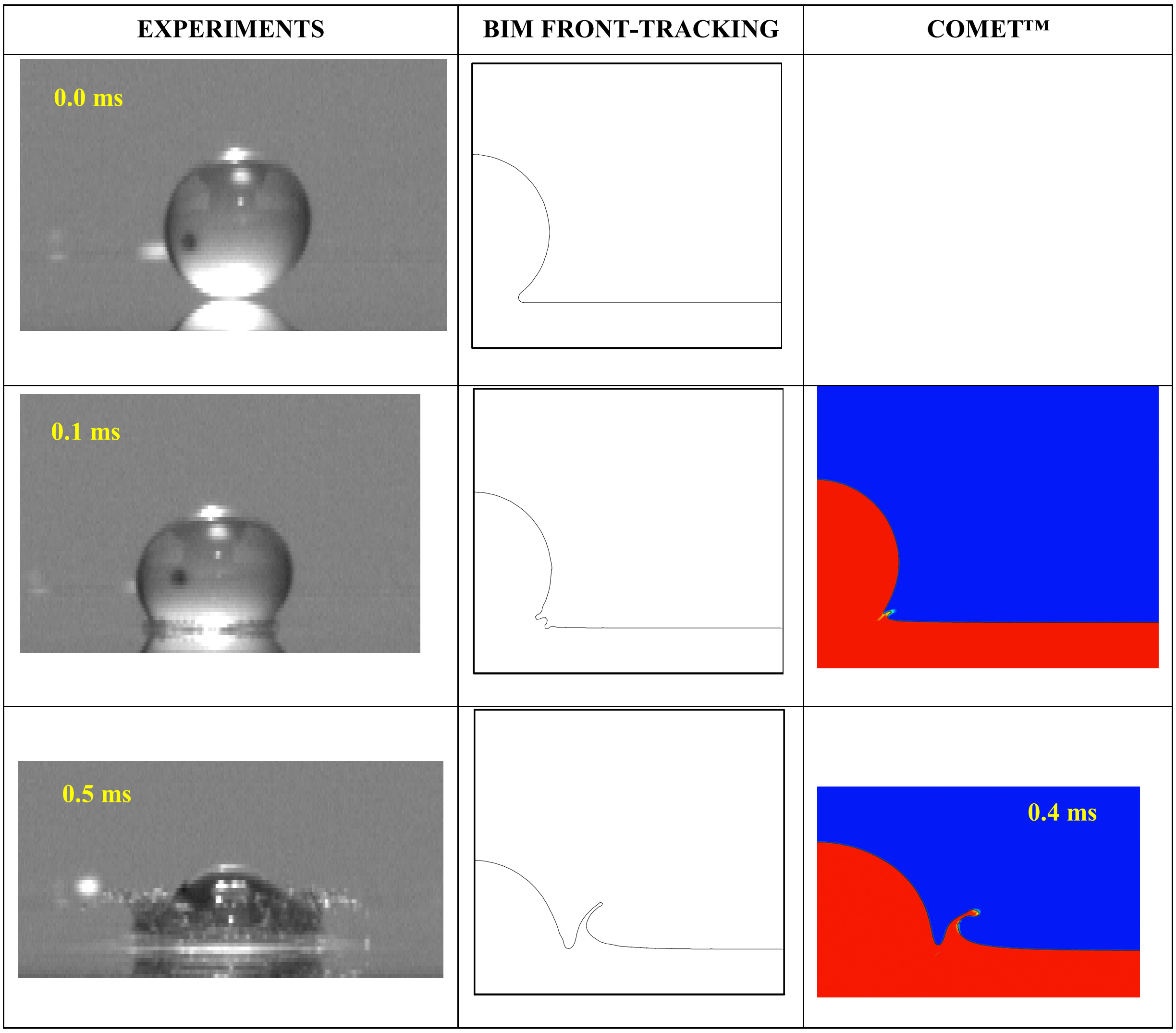

Figure 2. Comparison of experimental images depicting a 3.85mm water drop impinging with 3.05m/s on a 1.12mm-deep quiescent pool of water (left column) with BIM-based front-tracking computations (centre column) and front-capturing CFD computations (right column). (Continued next page)

From 0.5ms onward, the experimental images show the subsequent development of the crown, which exhibits secondary droplet ejection, or "splashing". Both axisymmetric flow models employed here cannot describe this phenomenon, which is known to be three-dimensional and depended upon the formation of fingers [3] along the rim of the crown (*also see* later times of Fig. 2). However, good qualitative agreement is demonstrated by both methods with regards to the rest of the basic attributes of the flow depicted by the images: the formation of a crown possessing the typical bent shape is predicted; its height is shown to increase with time, while its inclination with respect to the vertical gradually reduces; the formation of a rim on its edge is also captured; the rim grows with time. These trends have not been demonstrated by previous BIM computations [15].

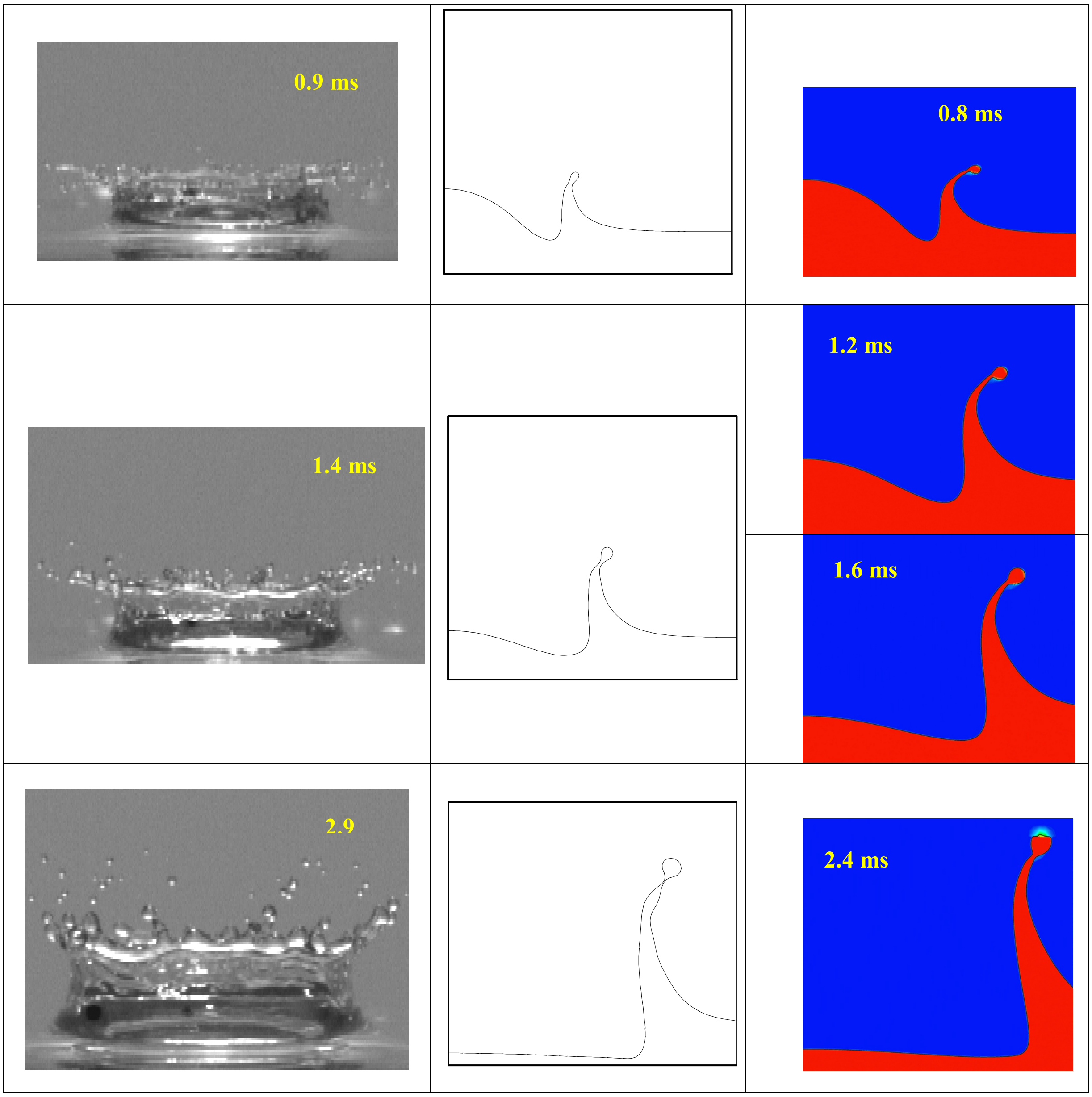

Figure 2 (cont'd). Comparison of experimental images depicting a 3.85mm water drop impinging with 3.05m/s on a 1.12mm-deep quiescent pool of water (left column) with BIM-based front-tracking computations (centre column) and front-capturing CFD computations (right column).

It is of interest to examine and compare in more detail the free-surface shapes predicted by the two flow-model/numerical-method approaches. Differences between the predicted shape, size and inclination of the computed crowns are evident. At intermediate times of 0.9ms and 1.4ms (*see* Fig. 2), the inclination and length of the *upper* parts of the crown predicted by the front-capturing computation seem to be in better qualitative agreement with the experiment than those predicted by the front-tracking computation. At the latest time of 2.9ms (*see* Fig. 2), additional topological details (surface undulations) appear on the outer wall of the crown predicted by the latter approach, while the respective crown predicted by the former method retains a smoother appearance. Although an amount of "waviness" is evident on the outer walls of the actual crown, it cannot be ascertained whether the BIM solution is indeed capturing this physical phenomenon or exhibits some form of artificial instability. A further notable difference concerns the apparent crown thickness in the immediate vicinity of the rim; the inviscid solution suggests it to be almost infinitesimal, while the viscous solution maintains a finite wall thickness (*see* last time of Fig. 2). Although the actual thickness of the crown is not discernible in the images, no tendency for rim detachment, as suggested by the BIM result, is yet evident.

On the other hand, similarities are evident in the regions of the solutions which concern the deforming drop and the *base* of the crown. The shapes of the *lower* inner and outer walls defining the latter, in particular, appear to be identical for the two different flow-model/numerical-method approaches, and additionally in good agreement with the experiment. This, in view of the flow assumptions adopted for the BIM computation, indicates that the effects of viscosity and vorticity during the evolution of the impingement event should be negligible in the lower regions of the flow.

Conclusions

A one-fluid, potential flow model, solved by a BIM-based front-tracking approach, proves capable of predicting the evolution of the typical topological features of the free-surface, as exhibited during the impingement of a drop onto a shallow liquid pool. The commercially-available CFD code tested, provides similar results. On a five years old HP workstation it requires at least 20 times greater CPU-time per timestep (5 times greater total computation time) than the BIM implementation on a Athlon based PC, also due to the relatively high grid resolution required to preserve acceptable interface sharpness [17]. This draws attention to the possible economy of the BIM approach. Machine-independent runs should be further performed to verify completely this result. The two model/method approaches yield solutions which depict identical free-surface shapes in most regions, except for the upper part of the crown where the two-fluid viscous model seems to give more realistic predictions. This suggests that the effects of viscosity on the evolution of the impingement event, for low viscosity liquids such as water, are important in the vicinity of the crown rim at least during the rising of the crown.

Acknowledgments

The work was partly financed by the British-Council-CRUI program (2001 and 2002) and by the Italian MIUR-PRIN2000 program under the contract MM09245595_005.

References

[1] Rein, M., “Phenomena of liquid drop impact on solid and liquid surfaces”, Fluid Dynamics Research 12, 61-93, (1993).

[2] Tropea, C., and Marengo, M., “The impact of drops on walls and films”, Multiphase Science and Technology 11, 19-36, (1999).

[3] Cossali, G.E., Coghe, A., and Marengo, M., “The impact of a single drop on a wetted solid surface”, Experiments in Fluids 22, 463-472, (1997).

[4] Ghielmetti, C., Marengo, M., Steigleder, T. and Tropea, C., “Droplet impingement on a solid surface covered by a liquid film”, 13th Annual Conference on Liquid Atomisation and Spray Systems, Florence, Italy, July 1997, pp. 465-471.

[5] Scardovelli, R., and Zaleski, S., “Direct numerical simulation of free-surface and interfacial flow”, Annual Review of Fluid Mechanics 31, 567-603, (1999).

[6] Uverdi, S.O., and Tryggvason, G., “A front tracking method for viscous, incompressible multi-fluid flows”, Journal of Computational Physics 100, 25-37, (1992).

[7] Blake, J.R., Taib, B.B., and Doherty, G., “Transient cavities near boundaries. Part 2. Free surfaces”, Journal of Fluid Mechanics 181, 197-212, (1987).

[8] Lundgren, T.S., and Mansour, N.N., “Oscillations of drops in zero gravity with weak viscous effects”, Journal of Fluid Mechanics 194, 479-510,(1988).

[9] Longuet-Higgins, M.S., and Cokelet, E.D., “The deformation of steep surface waves on water, I. A numerical method of computation”, Proceedings of the Royal Society of London A 350, 1-26,(1976).

[10] Stansby, P.K., Chegini, A., and Barnes, T.C.D., “The initial stages of dam-break flow”, Journal of Fluid Mechanics 374, 407-424, (1998).

[11] Pozrikidis, C., The Boundary Integral and Singularity Methods for Linearised Viscous Flow, Cambridge University Press, 1992.

[12] Oguz, H.N., and Prosperetti, A., “Surface-tension effects in the contact of liquid surfaces”, Journal of Fluid Mechanics 203, 149-171 (1989).

[13] Esmailizadeh, L., and Mesler, R., “Bubble entrainment with drops”, Journal of Colloid Interface Science 110, 561-574, (1986).

[14] Prosperetti, A., and Oguz, H.N., “The impact of drops on liquid surfaces and the underwater noise of rain”, Annual Review of Fluid Mechanics 25, 577-602, (1993).

[15] Weiss, D.A., and Yarin, A.L., “Single drop impact onto liquid: neck distortion, jetting, tiny bubble entrainment, and crown formation”, Journal of Fluid Mechanics 385, 229-254, (1999).

[16] Banerjee, P.K., The Boundary Element Methods in Engineering, McGraw-Hill, 1994.

[17] Marengo M., R. Scardovelli, C. Josserand and S. Zaleski, "Isothermal Drop-Wall Interactions. Introduction to experimental and numerical approaches", in “Navier Stokes Equations: Theory and Numerical Methods“, Marcel & Dekker Inc. (2001)